# Jointly Assimilating MODIS LAI and ET Products Into the SWAP Model for Winter Wheat Yield Estimation

Jianxi Huang, Hongyuan Ma, Wei Su, Xiaodong Zhang, Yanbo Huang, Jinlong Fan, and Wenbin Wu

***Abstract*—Leaf area index (LAI) and evapotranspiration (ET) are two crucial biophysical variables related to crop growth and grain yield. This study presents a crop model–data assimilation framework to assimilate the 1-km moderate resolution imaging spectroradiometer (MODIS) LAI and ET products (MCD15A3 and MOD16A2, respectively) into the soil water atmosphere plant (SWAP) model to assess the potential for estimating winter wheat yield at field and regional scales. Since the 1-km MODIS products generally underestimate LAI or ET values in fragmented agricultural landscapes due to scale effects and intrapixel heterogeneity, we constructed a new cost function by comparing the generalized vector angle between the observed and modeled LAI and ET time series during the growing season. We selected three parameters (irrigation date, irrigation depth, and emergence date) as the reinitialized parameters to be optimized by minimizing the cost function using the shuffled complex evolution method—University of Arizona (SCE-UA) optimization algorithm, and then used the optimized parameters as inputs into the SWAP model for winter wheat yield estimation. We used four data-assimilation schemes to estimate winter wheat yield at field and regional scales. We found that jointly assimilating MODIS LAI and ET data improved accuracy ($\mathbf{R^2 = 0.43}$, $\mathbf{RMSE = 619\ kg \cdot ha^{-1}}$) than assimilating MODIS LAI data ($\mathbf{R^2 = 0.28}$, $\mathbf{RMSE = 889\ kg \cdot ha^{-1}}$) or ET data ($\mathbf{R^2 = 0.36}$, $\mathbf{RMSE = 1561\ kg \cdot ha^{-1}}$) at the county level, which indicates that the proposed estimation method is reliable and applicable at a county scale.**

***Index Terms*—Data assimilation, evapotranspiration (ET), leaf area index (LAI), remote sensing, soil water atmosphere plant (SWAP) model.**

## I. Introduction

THE North China Plain has the largest wheat production in China. However, water stress has become the dominant limiting factor for wheat yield due to water shortages in the region. Consequently, accurate monitoring of regional wheat growth and yield estimation has become crucial for sustainable agricultural development and national food security. However, most yield prediction methods still depend on conventional techniques, such as predictions from agro-meteorological models and empirical statistical regression models that relate remotely sensed spectral vegetation indices and field-measured yields. One of the main drawbacks of such empirical models for estimating crop yields is that their application is only valid for specific crop cultivars, particular crop growth stages, or certain geographical regions [1], [2].

Previous studies have confirmed that mechanistic process-based crop simulation models can be successfully applied to simulate crop growth and estimate crop yield at a single point scale; however, practical regional application of such models is hampered by uncertainties in the model's structure and processes, and especially by uncertainties in the input parameters and initial conditions of the crop model. Thus, there is increasing interest in combining new methods to provide better estimates of model parameters and initial conditions at a regional scale with the goal of improving the simulation capabilities of crop growth models [3]. Because remotely sensed data offer the advantage of providing frequent, synoptic, and up-to-date overviews of actual crop growing conditions over large areas, remote sensing can be employed in conjunction with crop models to predict crop yield at a range of spatial scales [4]. Furthermore, remotely sensed data can be used to complement crop model simulations under situations that are not accounted for by the crop models [5], [6]. Therefore, the data assimilation technique has increasingly been applied to improve the simulation ability of crop models at large spatial scales [7], [8]. A number of studies have assimilated remote-sensing data into crop growth models to estimate crop yield with considerable success [8]–[11].

Most agricultural data assimilation studies have chosen leaf area index (LAI) as a unique state variable in crop growth models [12], [13] to estimate crop yield, with the simulation conducted in potential mode (i.e., based on the assumption that no other factors limit growth). Since other limiting factors (e.g., water stress, nutrient deficiencies, and pests) are not accounted for in the assimilation procedure, this leads to large estimation errors compared with field-measured crop yield. There have been several studies of bivariable assimilation, which attempts to account for more factors that affect growth, and there have

Manuscript received November 01, 2013; revised December 22, 2014; accepted January 28, 2015. Date of publication March 17, 2015; date of current version September 12, 2015. This work was supported by the National Natural Science Foundation Project of China under Grant 41371326. *(Corresponding author: Wei Su.)*

J. Huang, H. Ma, W. Su, and X. Zhang are with the College of Information and Electrical Engineering China Agricultural University, Beijing 100083, China, and also with the Key Laboratory of Agricultural Information Acquisition Technology, Ministry of Agriculture, Beijing 100083, China (e-mail: jxhuang@cau.edu.cn; suwei@cau.edu.cn).

Y. Huang is with the Agricultural Research Service, Crop Production Systems Research Unit, United States Department of Agriculture, Stoneville, MS 38776 USA.

J. Fan is with the National Satellite Meteorological Center, China Meteorological Administration, Beijing 100081, China.

W. Wu is with the Institute of Agricultural Resources and Regional Planning, Chinese Academy of Agricultural Sciences, Beijing 100081, China.

Color versions of one or more of the figures in this paper are available online at http://ieeexplore.ieee.org.

Digital Object Identifier 10.1109/JSTARS.2015.2403135

been some promising results. For example, Nearing *et al.* [14] assimilated remote-sensing observations of LAI and soil moisture into the decision support system for agro-technology transfer-cropping system model (DSSAT-CSM) CERES model [15] using an ensemble Kalman filter (EnKF) and a sequential-importance resampling filter. They found that the potential of assimilation to improve end-of-season yield estimates was low due to a lack of root-zone soil moisture information, errors in LAI observations, and the weak correlation between leaf and grain growth. Ines *et al.* [16] developed a data-assimilation (DA) framework for crop modeling that incorporated remotely sensed soil moisture and LAI into the DSSAT-CSM-Maize model using EnKF assimilation. They found that independent assimilation of LAI or soil moisture slightly improved the correlation between simulated and measured yield, but that the yield estimation improved greatly when soil moisture and LAI were assimilated simultaneously. These results indicated that bivariable assimilation has the potential to optimize crop parameters and state variables, thereby improving crop yield estimation.

In addition to LAI and soil moisture, evapotranspiration (ET) can be assimilated into crop models. Specifically, LAI and ET reflect two important crop physiological processes: 1) LAI simulates the crop's canopy development, which determines light interception and the potential for photosynthesis; 2) ET reflects the soil moisture level and thus, the water available to support plant growth; the ratio of actual to potential ET indicates the degree of soil water stress and thus, the magnitude of the constraint on plant growth. Improving the simulation of these two parameters can be critical for accurate crop yield estimation at both field and regional scales. Several previous studies have attempted to optimize the parameters of the SWAP model through ET assimilation using different remote-sensing datasets to adjust the relevant model parameters. However, most of the studies were based on the ET retrieved by the surface energy balance algorithm for land (SEBAL) model [17] based on data from the Landsat Thematic Mapper (TM). Irmak and Kamble [18] assimilated SEBAL-calculated ET into the SWAP model to estimate the uncertainty of the SWAP parameters by means of genetic algorithms. They input the optimized parameters into the SWAP model to estimate soil water-balance conditions and support on-demand irrigation scheduling. Vazifedoust *et al.* [19] developed a constant-gain Kalman filter DA algorithm to forecast total wheat production through assimilating remotely sensed LAI and/or relative ET, and found they could obtain a reasonably good prediction of yield 1 month in advance at a regional scale. Droogers *et al.* [20] assimilated ET values derived from Landsat TM data using the SEBAL algorithm to optimize the depth of irrigation using an automatic optimization program, and then applied a forward–backward approach to test the minimum return time of the satellite and the required accuracy of remotely sensed ET to permit accurate assessment of irrigation applications. They found that irrigation application could be estimated with reasonable accuracy. Charoenhirunyingyos *et al.* [21] combined the SWAP model with genetic algorithms to assimilate remotely sensed LAI, $\mathrm{ET}_a$ (actual ET), or both simultaneously by searching for the most appropriate sets of soil hydraulic parameters that could minimize the difference between the observed and simulated LAI or $\mathrm{ET}_a$, and found that different assimilation strategies could achieve high accuracy of soil moisture estimation at different soil depths. All of these previous studies demonstrated that ET is an important parameter in crop monitoring because it integrates the effects of multiple environmental factors (e.g., precipitation, temperature, and wind speed) with soil moisture conditions, which strongly influence crop functioning, development, and yield. Although soil moisture content would provide a more accurate reflection of water stress, it is difficult to determine by means of remote sensing once a crop covers the soil surface completely. In arid and semi-arid areas, it would be difficult both in theory and in practice to improve the performance of wheat yield estimation without assimilating information on levels of water stress. Remote-sensing-derived LAI and ET values are, therefore, important parameters for data assimilation because of their strong relationship with crop growth and thus, crop yield. Thus, assimilating both LAI and ET should offer advantages over single-variable assimilation strategies.

It can be challenging to assimilate data with coarse resolution such as the 1-km MODIS LAI and ET products into crop models, because these data tend to greatly underestimate the values compared to ground-based observations [22], [23]. This is due to a combination of the mixed-pixel effect (i.e., the low frequency of pixels that contain only the crop) and the heterogeneous land cover in most agricultural areas [24], [25]. In addition, there is often a mismatch in the spatial scale between remote-sensing observations and the crop model's state variables, so directly assimilating 1-km MODIS products values would introduce significant errors. There are two main solutions to reduce the scale effect. First, the parameter values retrieved by remote-sensing data or parameters used by the crop models can be scaled down or up,respectively, so that both use the same scale. Second, the temporal trends or phenological characteristics of the remote-sensing data can be assimilated into the crop model [26]; in this approach, the goal is to accurately capture the trends over time, which is particularly useful when the first approach is known to greatly overestimate or underestimate the field-measured values.

In this study, we chose the second approach and developed a crop model–data assimilation framework for assimilating the temporal variation obtained from MODIS ET and LAI data into a crop model to improve its ability to estimate crop yield at a regional scale. We then compared the model's estimation accuracy without data assimilation to the accuracy based on assimilation of one or both parameters. Despite the obvious underestimation of field values by the MODIS LAI [23], [24] and ET [27], [28] products in regions where winter wheat is planted, these two products can accurately capture the temporal variation in relatively pure pixels. Thus, the objectives of this study were as follows:

1) to evaluate the potential use of a time series of 1-km MODIS ET and LAI products for the estimation of regional winter wheat yield;
2) to investigate whether jointly assimilating the MODIS ET and LAI products performed better than assimilating each of these parameters individually.

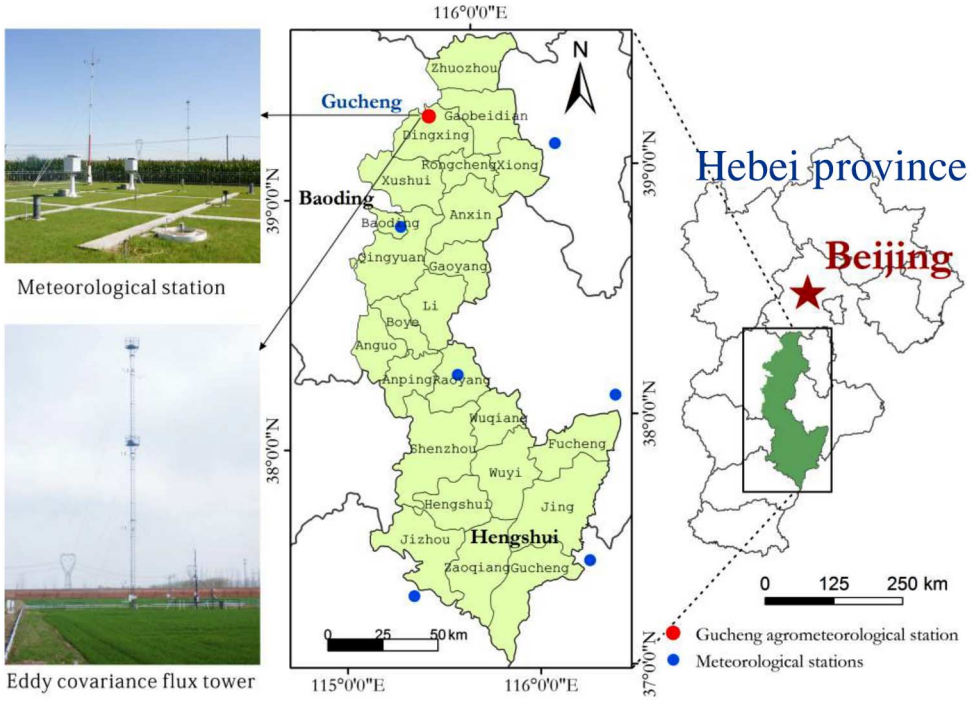


Fig. 1. Location of the study area, of the meteorological stations, and of the 24 counties in the study area in southern Hebei Province.

## II. Materials and Methods

### A. Study Area

The study was implemented in a planted area dominated by winter wheat in the Baoding and Hengshui districts (115°10′E to 116°34′E, 37°03′N to 39°36′N) of southern Hebei Province, China (Fig. 1), covering 16 335 $km^2$ in total and consisting of 24 counties. The prevailing cropping pattern is winter wheat in rotation with summer corn. In general, the topography of the region is characterized by alluvial plains with gently rolling topography. The regional climate is a continental monsoon with an average annual rainfall ranging from 400 to 800 mm and an average temperature ranging from 9°C to 15°C. In 2009, we obtained data for the seven key phenological stages of winter wheat: 1) green-up (early March); 2) jointing (late March); 3) elongation (early April); 4) booting (late April); 5) heading (early May); 6) anthesis (middle May); and 7) maturity (early June). Fig. 1 shows the locations of the meteorological stations used to obtain climate data for the study area. Based on observations during the past 30 years at the Luancheng Agro-Ecosystem Experimental Station of Chinese Academy of Sciences, which is situated only 50 km from our study area, the actual ET of irrigated farmland in this region is between 800 and 900 mm annually (i.e., rainfall is much less than the actual ET), and an average of 350 mm of groundwater must be extracted annually to cover the water deficiency [29]. Thus, timely irrigation during crucial phenological stages is important to guarantee high wheat yield in this region.

### B. SWAP Model

SWAP is a comprehensive agro-hydrological model for analyzing the interactions among soil, water, atmosphere, and plants. It was developed by the Wageningen University and Research Center (Wageningen, the Netherlands). The SWAP model includes a growth simulation module (WOFOST 6.0) to simulate crop growth. The WOFOST model provides estimates of biomass and grain yield at a daily time step for different crop types. The simulation results are directly usable for qualitative crop-specific assessment of the growing season and for crop yield estimation. SWAP also offers a powerful ability to simulate the soil water balance, which can be used to enhance the weaker simulation provided by the WOFOST module. Potential ET in the SWAP model is calculated using the Penman–Monteith equation [30]. The actual ET is calculated by applying a factor that accounts for the reduction in root water uptake caused by water or salinity stress to adjust the potential ET. The ratio of actual to potential ET is used to quantify the degree of water stress and its impact on crop growth. The SWAP model can be implemented in potential mode (based on the assumption of no constraints imposed by water availability) and water-limited mode. The difference in yield between the potential and water-limited modes can be interpreted as the net effect of soil water stress. Given the aridity and water shortages in the study area, we used the water-limited mode of SWAP in this study. The effects of nutrient deficiencies, pests, weeds, and diseases on crop growth and yield have not yet been simulated in the current version (3.0.3) of the SWAP model, so we did not account for these factors.

### C. SWAP Model Calibration

The SWAP model requires weather, soil, crop, and management parameters for each cell in the grid to simulate crop yield. Before a crop model can be implemented in a given agro-environment, calibration and performance evaluation must

be done to ensure that the model can accurately simulate the entire crop growth process by accounting for the variability of the parameters that characterize the crop model. In the present study, we calibrated the SWAP model for wheat cultivar "Hengguan 35" at the Gucheng experiment station (Fig. 1). An automated weather station installed for long-term observations at this site measures daily maximum and minimum temperatures, solar radiation, wind speed, actual vapor pressure, and precipitation. These variables were used to drive the SWAP model at the field scale. For complete details of calibration of the SWAP model for the study area, refer to our previous work [13], [31].

We performed a global sensitivity analysis using the extended Fourier amplitude sensitivity test method [32] to analyze the parameters that the SWAP model was most sensitive to, with the goal of identifying the most important parameters to be optimized. Using the Simlab software (version 2.2, Joint Research Centre, Ispra, Italy), we obtained the sensitivity of the SWAP model to ET and LAI. We found that the irrigation schedule and emergence date were very sensitive to daily ET and LAI and greatly affected the final yield. In addition, less sensitive parameters are fixed structural parameters of the soil that cannot be adjusted and variables such as the soil evaporation coefficient have a physical meaning and must be calculated based on field experiments. Initial parameters such as the emergence date, minimum temperature at which growth begins, and initial total crop dry weight generally vary across large spatial regions, which makes it difficult to acquire accurate values of these parameters at the regional scale. Therefore, we chose three parameters to which the model was sensitive based on the global sensitivity analysis (irrigation date, irrigation depth, and emergence date) as the parameters to be optimized in the assimilation procedure.

To implement the SWAP model at a regional scale, the spatial distribution of the climate data from various meteorological stations must be determined. In this study, we used a common Kriging interpolation routine in ArcGIS 9.3 to estimate the values of weather variables for each $10\,\mathrm{km} \times 10\,\mathrm{km}$ grid cell, including daily maximum and minimum temperatures, solar radiation, wind speed, and actual vapor pressure. For precipitation, we used a daily gridded precipitation dataset with $25\,\mathrm{km} \times 25\,\mathrm{km}$ cells that we obtained from the China meteorological data sharing service system (http://cdc.cma.gov.cn/).

### D. Field-Measured Data

Half-hourly eddy covariance data from the flux tower at the Gucheng experiment station (Fig. 1) was used to calibrate and validate the ET assimilation at a field scale. The eddy covariance technique is a widely used method to measure ecosystem mass and energy fluxes [25]. Since the data obtained from the flux tower is the latent heat flux, which is the equivalent of the energy used in the description of the ET process, it must be converted to the same time step as the instantaneous ET. Actual instantaneous *ET* ($\mathrm{mm\ day^{-1}}$) was calculated as follows:

$$ET = \frac{86\,400 \times 1000}{\rho_w \lambda} LE \tag{1}$$

where *LE* is latent heat flux ($\mathrm{W \cdot m^{-2}}$), $\rho_w$ is the density of water ($\mathrm{kg \cdot m^{-3}}$), and $\lambda$ is the latent heat of vaporization ($\mathrm{J \cdot kg^{-1}}$), and there are 86 400 s in a day and 1000 mm in 1 m. The latent heat of vaporization can be calculated from the air temperature, but we have used constant values for $\rho_w$ and $\lambda$, so (1) can be simplified into

$$ET = 0.0351\ LE. \tag{2}$$

This equation converts the latent heat flux into an equivalent daily ET. Since the flux data were available at half-hour intervals, the daily ET for day $i(ET_i)$ can be obtained as follows:

$$ET_i = \frac{1}{N} \sum_{j=1}^{N} ET^j_{30\,\mathrm{min}} \tag{3}$$

where $ET_j$ is the $j$ th 30-min observation on day $i$, and $N$ is the number of 30-min measurements of LE, which is usually 48 per day. When $N$ was less than 40, we considered the data quality unacceptable and did not include it in our analysis.

To capture the growth conditions for winter wheat at a regional scale, we selected 29 sample plots representing different winter wheat growing conditions throughout the study area and monitored the plots from March to June 2009. We manually measured winter wheat yields in these plots before harvesting in mid-June, and obtained county-level wheat yield data for the 24 counties in the study area from Hebei statistical yearbook in 2009.

### E. Crop Type Map Derived From Landsat TM

We acquired six Landsat TM scenes of the study area during the winter wheat growing season (on March 14, May 17, and June 2, 2009, during the green-up, filling, and maturity stages, respectively). The TM images were geo-referenced to the Albers conical equal area map projection using field-measured ground control points. After geometric correction, the root-mean-square error (RMSE) of the location was smaller than one pixel (30 m) for each TM image. An atmospheric correction was applied using the fast-line-of-sight atmospheric analysis of spectral hypercubes (FLASSH) atmospheric correction module of the ENVI software (Version 5.1, Exelis Visual Information Solutions, http://www.exelisvis.com) to obtain the reflectance value in each TM band. We obtained the spatial distribution of crop types in the study area using the Mahalanobis distance algorithm provided by the ENVI software based on supervised classification of the three TM images. We used the resulting map to mask out all pixels that were not classified as winter wheat fields, most of which represented cotton, other crops, buildings, bare soil, trees, and water. Fig. 2(a) shows the resulting crop type map. We overlaid the 30-m crop type map on a 1-km grid so that we could calculate the pixel purity (i.e., the percentage of winter wheat in each cell of the grid. The winter wheat pixels with the highest purity were mostly located in the middle of the study area [Fig. 2(b)]. In our subsequent assimilation procedure, we only included grid cells with at least 50% winter wheat to reduce the influence of other types of land cover on the analysis.

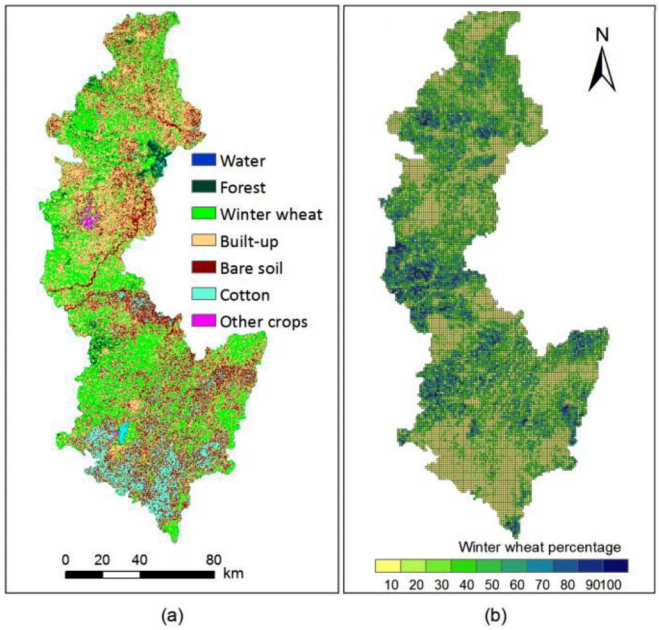


Fig. 2. (a) Land use map at a 30-m resolution and (b) winter wheat purity map at a 1-km resolution.

### F. MODIS ET and LAI Products

The MOD16 global ET product is part of the National Aeronautics and Space Administration Earth Observing System (NASA/EOS) project to estimate global terrestrial ET using satellite data. The MOD16 ET datasets are estimated using an improved ET algorithm based on the Penman–Monteith equation [25], [27]. In the present study, we used the 8-day MODIS ET product (http://www.ntsg.umt.edu/project/mod16).

We used the 1-km 4-day MODIS LAI product (MCD15A3) to cover the majority of the growing season from January to June 2009 (http://reverb.echo.nasa.gov/reverb). Due to the presence of cloud or atmospheric contamination, the MODIS LAI profiles did not present a smooth and continuous series. Thus, we applied the Savitzky–Golay filtering algorithm to smooth the MODIS LAI profile in each winter wheat pixel [13], [33].

### G. Data Assimilation Scheme

The SWAP–SCE scheme combines the SWAP model with the shuffled complex evolution method–University of Arizona (SCE-UA) algorithm to take advantage of the optimization algorithm for determining the reinitialized parameters using the time series of satellite-derived LAI and ET values. The goal is to minimize a cost function. Uncertain input parameters in SWAP, such as irrigation parameters and the emergence date, were optimally estimated by assimilating the temporal variations of the MODIS LAI and ET into the SWAP model through an iterative process. The SWAP–SCE scheme was then implemented until we obtained the best fit between the model simulations and the satellite observations ($ET_a$ and LAI, independently or in combination). Crop yield is the major output of the SWAP model. After completing the assimilation procedure for all of the 1-km cells containing at least 50% wheat, we aggregated the yield at a county level by using an area-weighted average yield. Finally, we compared these estimates with official county-level statistics to evaluate the performance of the data assimilation. Fig. 3 illustrates the overall assimilation procedure in the SWAP-SCE scheme.

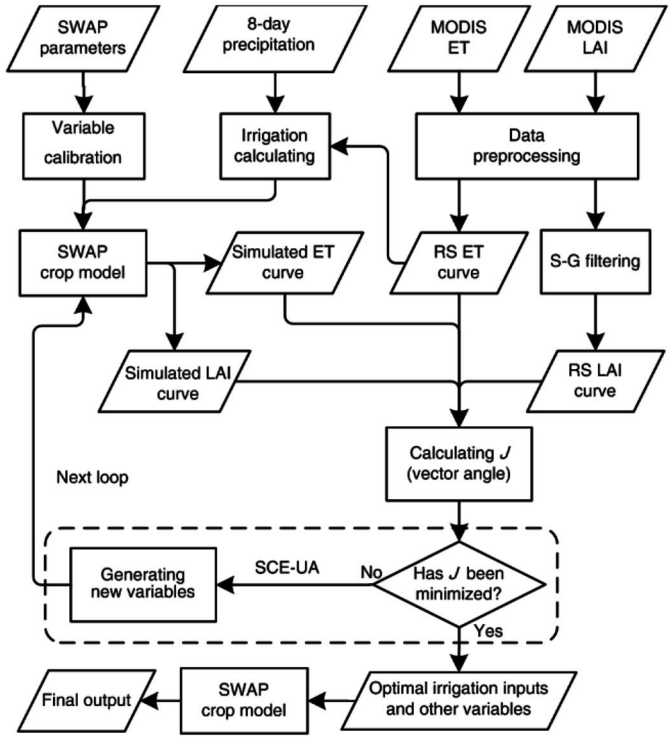


Fig. 3. Flowchart showing the ET and LAI assimilation procedures used in the SWAP-SCE scheme. RS, remote sensing; S–G, Savitzky–Golay filtering.

*1) Selection of Reinitialized Parameters for the SWAP Model:* Several studies indicate that LAI is sensitive to the initial dry biomass of the crop (TDWI) and the emergence date (IDEM) [5], [31], and that the latter parameters can be used as the reinitialized parameters in the assimilation procedure. Precipitation and irrigation are two key variables that determine crop ET. Accurate precipitation data can be obtained from weather stations, and an optimal interpolation algorithm can be applied to generate a map of the precipitation distribution. However, regional cropland irrigation data are usually difficult to obtain due to the high variability of agricultural irrigation activity. MODIS ET products can compensate for these problems by providing the integrated result of precipitation and irrigation in cropland. Based on our previous work [31], we selected three parameters that LAI, ET, and yield were sensitive to (emergence date, irrigation date, and irrigation depth) at two phenological stages for the irrigation data (heading and filling). These five parameters were calibrated and adjusted using the DA strategy. The initial values and ranges of values for the five parameters are shown in Table I. The crop emergence date and the irrigation data during the two stages were estimated from day of year (DOY) 60 to DOY 150 during the assimilation procedure. The specific date and depth of irrigation in the SWAP model for each cell in the grid that contained at least 50% winter wheat were determined through the data assimilation procedure.

TABLE I
LISTS OF PARAMETERS THAT WERE OPTIMIZED

| Parameter | Initial value | Range of values |
|---|---|---|
| Emergence date | 22 October | 7 October to 6 November |
| Irrigation date 1 | DOY 100 | DOY 60 to DOY 120 |
| Irrigation date 2 | DOY 120 | DOY 90 to DOY 150 |
| Irrigation depth 1 | 9.05 cm | 0 to 30 cm |
| Irrigation depth 2 | 9.05 cm | 0 to 30 cm |

*2) Construction of the Cost Function:* The SCE-UA algorithm is a general-purpose global optimization procedure [34]–[36]. It was designed to deal with the specific types of problems encountered in the calibration of a conceptual watershed model, but has been successfully used for optimization in other fields of study [37], [38].

The traditional cost function, which is determined using the least-squares method, assumes that the observations are accurate and unbiased. However, observational data usually contains inaccuracies and biases that will introduce new errors when using the least-squares method and decrease its effectiveness. To avoid this problem, we developed a new cost function by comparing the generalized vector angles of the model output and the observation profile at 8-day intervals for the ET data and 4-day intervals for the LAI data. This method has not previously been used in DA analyses. The computational procedure can be described as follows.

First, the generalized vector angle of the remotely sensed data and the model simulations were calculated, and the positive and negative values of the first differential were calculated. We then calculated the sum of the generalized vector angles from the LAI and ET time series, which we used to represent the cost function's value:

$$\theta = \arccos \frac{\sum_{i=1}^{n} x_i \cdot y_i}{\sqrt{\sum_{i=1}^{n} {x_i}^2} \sqrt{\sum_{i=1}^{n} {y_i}^2}}, \quad \theta \in \left[0, \frac{\pi}{2}\right] \tag{4}$$

where $\theta$ denotes the vector angle between the two profiles, $x_i$ denotes the value from the MODIS LAI or ET time series at time $i$, $y_i$ denotes the SWAP-simulated value from the LAI or ET time series at time $i$, $n$ represents the number of observations for ET and LAI, and $\pi$ is the constant 3.14. Because the inverse cosine calculation does not change the monotonicity of the original function, we eliminated this calculation to improve the computation efficiency. The final cost function is

$$J = \frac{\sqrt{\sum_{i=1}^{n} \mathrm{obsLAI}_i{}^2} \sqrt{\sum_{i=1}^{n} \mathrm{simuLAI}_i{}^2}}{\sum_{i=1}^{n} \mathrm{obsLAI}_i \cdot \mathrm{simuLAI}_i} + \frac{\sqrt{\sum_{j=1}^{m} \mathrm{obsET}_i{}^2} \sqrt{\sum_{j=1}^{m} \mathrm{simuET}_i{}^2}}{\sum_{j=1}^{m} \mathrm{obsET}_i \cdot \mathrm{simuET}_i} \tag{5}$$

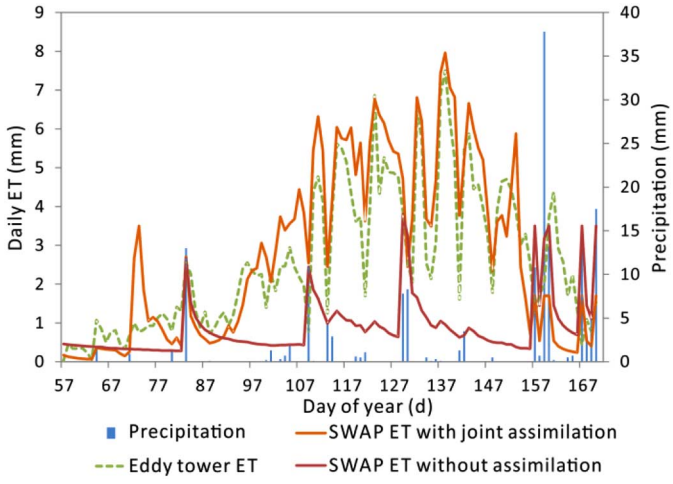


Fig. 4. Comparisons of the ET profiles with and without data assimilation at the Gucheng station.

where the prefix "obs" means the observed MODIS ET or LAI values, the prefix "simu" means the SWAP-simulated values of ET or LAI, and $m$ and $n$ denote the number of observations for ET and LAI, respectively.

If $\theta = 0$, this means that the curves of the MODIS LAI or ET and the SWAP-simulated LAI or ET time series would have identical shapes, and the values in the time series at any given time are proportional; in contrast, the two data sequence are orthogonal to each other when $\theta = \pi/2$.

## III. RESULTS

### *A. Assimilating the MODIS ET and LAI Values Into the SWAP Model at a Field Scale*

We assimilated the MODIS ET and LAI values into the SWAP model based on data from the Gucheng station at a field scale. We compared the SWAP-simulated ET with and without data assimilation with values at the Gucheng flux tower at a daily scale throughout the main growing season from DOY 57 to DOY 169 at the field scale (Fig. 4). We optimized the five reinitialized parameters by minimizing the cost function using the SCE-UA algorithm. We found that the assimilated ET has a good agreement with the temporal variations in crop ET recorded at the flux tower. During the period of decreasing growth (DOY 120–167), the values of the assimilated ET agreed well with those from the flux tower. However, the assimilated ET was higher than the flux tower ET during the period with increasing growth (DOY 57–120). This may have resulted from uncertainty in the soil and hydraulic parameters of the SWAP model, which would lead to a poor soil evaporation simulation when the soil is not fully covered by the winter wheat canopy. The SWAP-simulated ET without assimilation was much lower than the flux tower ET, possibly due to the lack of accurate irrigation data during the growing season. It is difficult for the SWAP model to accurately simulate the ET time series without accurate values for the irrigation parameters. A previous study [18] also suggested that irrigation had a major effect on cropland ET. In the absence of accurate irrigation

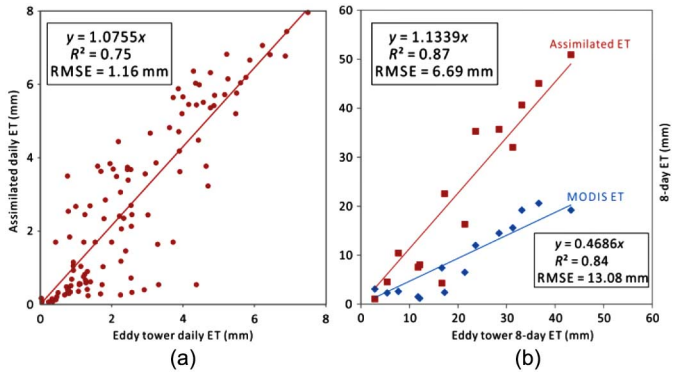


Fig. 5. Scatterplots of (a) daily and (b) 8-day ET values between the values simulated using data assimilation and flux tower ET at the Gucheng station. Only statistically significant regressions are shown.

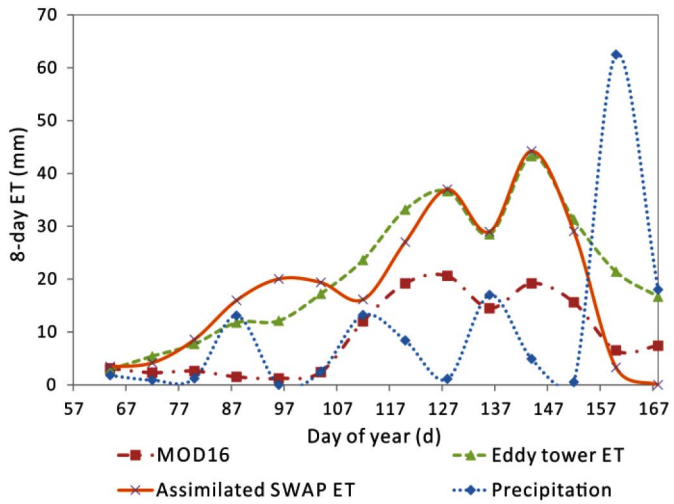


Fig. 6. Comparisons of 8-day cumulative ET profiles at the Gucheng station with and without data assimilation.

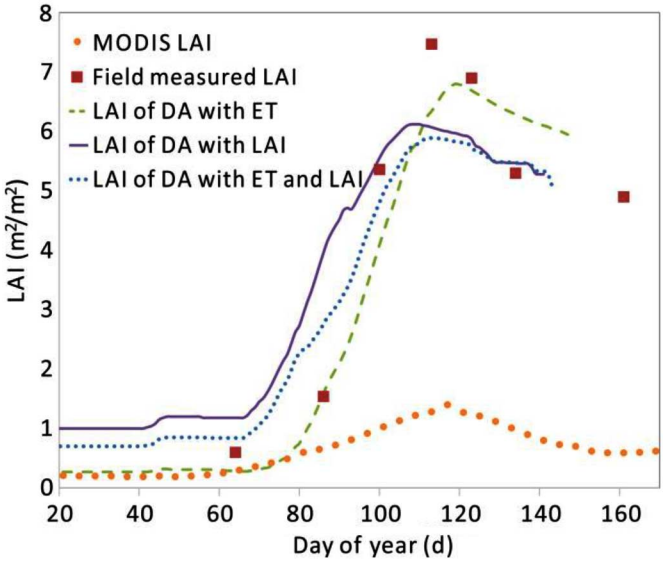


Fig. 7. Comparisons of the LAI profile with different assimilation schemes.

TABLE II
COMPARISONS OF THE ASSIMILATED WHEAT YIELD USING FOUR DA SCHEMES

| Scheme | Average yield ($kg \cdot ha^{-1}$) | Min ($kg \cdot ha^{-1}$) | Max. ($kg \cdot ha^{-1}$) | $R^2$ | RMSE ($kg \cdot ha^{-1}$) | $P$ |
|---|---|---|---|---|---|---|
| Without DA | 5930 | 5361 | 6686 | 0.03 | 433 | 0.394 |
| DA with LAI | 5127 | 4420 | 5892 | 0.28 | 889 | 0.010 |
| DA with ET | 5391 | 3130 | 6594 | 0.36 | 1561 | 0.004 |
| DA with both LAI and ET | 5730 | 4323 | 6697 | 0.43 | 619 | 0.001 |
| Least-squares cost function for DA | 3802 | 3024 | 5517 | 0.19 | 2289 | 0.042 |

parameters, the dominant water input was precipitation, which tends to produce lower crop ET values.

We performed linear regression to compare the daily and 8-day SWAP-simulated ET with data assimilation and the corresponding flux tower ET (Fig. 5). The results show a strong and significant relationship between the daily values ($R^2 = 0.75$, $\mathrm{RMSE} = 1.16\,\mathrm{mm}$). We also found that the mean absolute error (MAE) compared with the daily flux tower ET decreased from $1.9\,\mathrm{mm\ day^{-1}}$ to $0.91\,\mathrm{mm\ day^{-1}}$ compared with the SWAP-simulated ET without assimilation. To evaluate the accuracy improvement compared with the MOD16 ET, we converted the daily SWAP-simulated ET outputs into the 8-day values. The resulting ET estimates showed greatly improved accuracy (Fig. 6), with $R^2 = 0.87$ between the assimilated ET and the flux tower ET and $R^2 = 0.84$ between the assimilated ET and the MOD16 ET. (Note that although the RMSE values are higher than in the daily comparison, these values are for 8 days rather than 1 day.) Generally, the assimilated ET overestimated the flux tower ET but underestimated the MOD16 ET.

Although the MOD16 ET was lower than the flux tower observations, MOD16 ET provides a good representation of the temporal variations in ET throughout the growing season. The underestimation can be explained by the difference in the measured spatial scales and the associated variation in the cover types. Although the flux tower at the Gucheng station is surrounded by farmland, the MOD16 products have a 1-km spatial resolution, so they include buildings and roads within a pixel that would inevitably decrease the ET value. In contrast, the flux tower is surrounded by a 25-ha area of crops.

We assimilated the MODIS LAI and ET time series into the SWAP model and compared the resulting LAI profiles at the Gucheng station at a field scale (Fig. 7). The LAI profile based on assimilating only LAI closely followed the field-measured values, which indicates that assimilating LAI based on the generalized vector angle cost function effectively represented winter wheat's phenological conditions. It seems that assimilating only ET did not accurately reflect the crop's phenological characteristics, especially during the period of decreasing growth, when the LAI values remained too high. However, assimilating both LAI and ET achieved a balanced result between proper phenological timing and accurate LAI values.

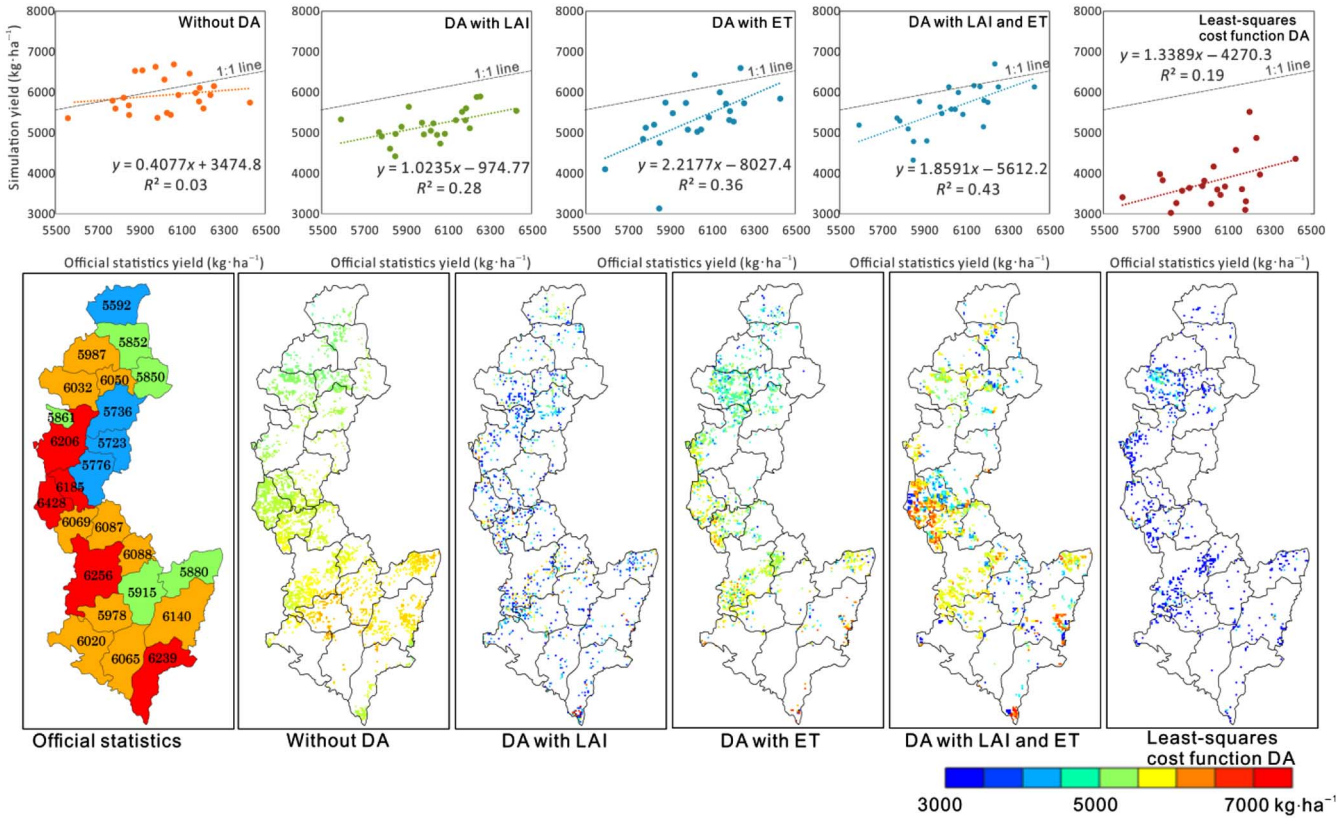


Fig. 8. (Top) Scatterplots of the relationship between the official and simulated wheat yield, and (bottom) maps of the yield spatial distribution without assimilation and with four DA schemes. All regressions were statistically significant.

At the Gucheng station, the optimized emergence date was October 30, 2008, the optimized irrigation dates were DOY 97 and DOY 123, and the corresponding irrigation depths were 3.4 and 9.5 cm in the data assimilation, and this provides guidance for determining the actual irrigation schedule. In addition to the optimized irrigation schedule, we also designated a fixed irrigation on DOY 151 with a depth of 12 cm. In the study area, winter wheat usually needs irrigation to meet its water requirements, and the total irrigation amount ranges from 30 to 460 mm; this would require two to six irrigations during the growing season [39]. Thus, the estimated irrigation amount is fairly high and the assimilated ET was higher than the flux tower measurements. There was also a strong correlation between the flux tower ET and the assimilated ET. These results show that data assimilation can substantially increase the accuracy of ET simulation by optimizing the irrigation parameters.

### *B. Assimilating the MODIS ET and LAI Products Into the SWAP Model at a Regional Scale*

We applied the DA procedure to the 1-km cells in the grid that had at least 50% winter wheat using the generalized vector angle cost function to optimize the irrigation parameters and emergence date, and aggregated the simulated wheat yield at a county level to allow validation of the results using official regional yield statistics, which are compiled at a county level. The simulated yield obtained using the SWAP model without data assimilation was quite accurate compared to the official yield statistics, with $\mathrm{RMSE} = 433\,\mathrm{kg}\cdot\mathrm{ha}^{-1}$, but the regression was not statistically significant ($R^2 = 0.03$, $p = 0.394$), since many factors other than weather affect crop yield in this semi-arid region. As a result, the irrigation schedule and other spatially heterogeneous parameters should be calibrated or optimized to better simulate the spatial distribution of yield at the regional scale.

We compared the results at a regional scale without assimilation with the results provided by four DA schemes (Table II): assimilation with ET alone, with LAI alone, with both ET and LAI, and with a least-squares cost function. The assimilation with both ET and LAI achieved the highest accuracy, with the highest $R^2$ (0.43) and the lowest RMSE ($619\,\mathrm{kg}\cdot\mathrm{ha}^{-1}$) among the statistically significant results. The spatial variability of the wheat yield in the assimilation using both ET and LAI also showed good agreement with the official wheat yield statistics at the county level due to the higher spatial detail of the optimized parameters (Fig. 8, Table III). In particular, the mid-western part of the study area [which had a concentration of pixels with high purity for winter wheat; Fig. 2(b)] had higher average yields than the northern regions. Generally, yield variability results from differences in solar radiation, temperature, and farming management (e.g., irrigation and fertilization).

Assimilating either LAI or ET alone improved the correlation with official wheat yield statistics (with $R^2$ of 0.28 and 0.36, respectively, both $p < 0.05$) compared to the SWAP results without assimilation ($R^2 = 0.03$, not significant). However,

TABLE III
COMPARISONS OF THE SIMULATED WHEAT YIELD WITHOUT ASSIMILATION AND USING FOUR DA SCHEMES BASED ON COUNTY-SCALE STATISTICS

| County | Official statistics yield | SWAP without DA | Relative error (%) | DA with LAI alone | Relative error (%) | DA with ET alone | Relative error (%) | DA with both LAI and ET | Relative error (%) | Least-squares method | Relative error (%) |
|---|---|---|---|---|---|---|---|---|---|---|---|
| Zhuozhou | 5592 | 5360.68 | –4.14 | 5328.44 | –4.71 | 4100.89 | –26.67 | 5343.67 | –4.44 | 3406.89 | –39.08 |
| Gaobeidian | 5852 | 5438.86 | –7.06 | 4970.45 | –15.06 | 4747.83 | –18.87 | 4954.22 | –15.34 | 3265.50 | –44.20 |
| Dingxing | 5987 | 5368.84 | –10.33 | 4956.95 | –17.20 | 5077.23 | –15.20 | 5716.94 | –4.51 | 3817.61 | –36.23 |
| Xushui | 6032 | 5491.13 | –8.97 | 5232.83 | –13.25 | 5023.35 | –16.72 | 6225.21 | 3.20 | 4165.43 | –30.94 |
| Xiong | 5850 | 5676.33 | –2.97 | 4420.00 | –24.44 | 3130.00 | –46.50 | 4616.43 | –21.09 | < 3000 | – |
| Rongcheng | 6050 | 5440.22 | –10.08 | 4947.86 | –18.22 | 5078.95 | –16.05 | 5769.04 | –4.64 | 3598.50 | –40.52 |
| Anxin | 5736 | 5597.62 | –3.26 | 4907.02 | –15.19 | 5123.04 | –11.46 | 5698.46 | –1.51 | 3829.66 | –33.81 |
| Qingyuan | 6206 | 5599.75 | –9.77 | 5110.23 | –17.66 | 5276.69 | –14.97 | 6213.03 | 0.11 | 5517.00 | –11.10 |
| Gaoyang | 5723 | 5790.96 | 0.31 | 5013.29 | –13.16 | 4846.00 | –16.06 | 5506.71 | –4.61 | 3979.17 | –31.07 |
| Li | 5776 | 5865.49 | 0.68 | 4606.18 | –20.94 | 5198.20 | –10.78 | 5124.11 | –12.05 | 3024.00 | –48.09 |
| Boye | 6185 | 5771.83 | –6.68 | 5308.85 | –14.17 | 5313.75 | –14.09 | 5278.48 | –14.66 | 3095.00 | –49.96 |
| Anguo | 6428 | 5743.74 | –10.64 | 5540.13 | –13.81 | 5839.79 | –9.15 | 6430.59 | 0.04 | 4357.03 | –32.22 |
| Raoyang | 6087 | 5931.43 | –2.56 | 4973.77 | –18.29 | 5378.75 | –11.64 | 5794.96 | –4.80 | 3672.00 | –39.67 |
| Anping | 6069 | 5980.69 | –3.05 | 5516.15 | –10.58 | 5717.07 | –7.33 | 6251.21 | 1.33 | 3606.64 | –41.54 |
| Shenzhou | 6256 | 6149.43 | –1.70 | 5892.96 | –5.80 | 5728.69 | –8.43 | 6333.46 | 1.24 | 3970.68 | –36.53 |
| Wuqiang | 6088 | 6107.17 | –1.31 | 5603.21 | –9.45 | 5536.53 | –10.53 | 6077.52 | –1.79 | 3309.44 | –46.52 |
| Fucheng | 5880 | 6527.52 | 11.01 | 5149.93 | –12.42 | 5744.40 | –2.31 | 5283.33 | –10.15 | 3569.45 | –39.29 |
| Wuyi | 5915 | 6539.34 | 10.56 | 5640.83 | –4.64 | 5483.00 | –7.30 | 5064.50 | –14.38 | 3637.67 | –38.50 |
| Jing | 6140 | 6456.83 | 5.16 | 5310.56 | –13.51 | 5996.80 | –2.33 | 5898.17 | –3.94 | 4574.89 | –25.49 |
| Hengshui | 5978 | 6627.65 | 10.87 | 5249.44 | –12.19 | 5735.37 | –4.06 | 6099.50 | 2.03 | 3685.31 | –38.35 |
| Jizhou | 6020 | 6310.96 | 4.83 | 5048.69 | –16.13 | 6429.36 | 6.80 | 6437.92 | 6.94 | 3244.67 | –46.10 |
| Zaoqiang | 6065 | 6686.25 | 10.24 | 4731.94 | –21.98 | < 3000 | – | 5595.75 | –7.74 | 3468.00 | –42.82 |
| Gucheng | 6239 | 5932.42 | –4.91 | 5882.48 | –5.71 | 6594.60 | 5.70 | 6140.35 | –1.58 | 4870.00 | –21.94 |
| Mean RE | | | 6.13 | | 13.85 | | 12.86 | | 6.18 | | 37 |

since the optimization procedure resulted in high variation of reinitialized parameter, it could not improve the accuracy of the yield estimation, and error levels were relatively high (RMSE = 889 and 1561 $\mathrm{kg \cdot ha^{-1}}$, respectively). The largest error in the estimated yield was obtained using the least-squares cost function ($R^2 = 0.19$; RMSE = 2289 $\mathrm{kg \cdot ha^{-1}}$). This can be explained by the fact that the low MODIS LAI values forced the SWAP model to reach unrealistically low wheat yield values using the least-squares cost function.

We calculated the relative error (RE) as follows to evaluate the accuracy of the yield estimates using the different DA schemes:

$$\mathrm{RE} = [(\text{Simulated yield} - \text{Official statistical yield})/ \text{Official statistical yield}] \times 100\%. \quad (6)$$

Table III summarizes the results. Assimilation using LAI or ET alone increased the error in the estimated wheat yield, with large mean RE values of 13.85% and 12.86%, respectively. Jointly assimilating both ET and LAI significantly decreased the mean RE to 6.18%. Especially for Qingyuan and Anguo counties, RE decreased to 0.1% and <0.1%, respectively, compared with the values obtained using SWAP without assimilation (–9.8% and –10.6%, respectively). However, several counties (e.g., Xiong, Gaobeidian, Boye, and Li counties) had higher RE than the value predicted by SWAP without assimilation. This may have been caused by the low planted density of winter wheat and more heterogeneous agricultural landscapes in these counties [Fig. 2(b)]. The coarse 1-km MODIS pixels also contained many non-wheat land cover types, which would increase the errors in the MODIS LAI and ET products. These results suggest that the accuracy of the reconstruction of temporal trends in LAI and ET derived from remote sensing strongly affects the performance of the generalized vector angle cost function.

## IV. DISCUSSIONS

Coarser pixels, such as those in the 1-km MODIS reflectance data, usually result in LAI or ET values that are obtained from more heterogeneous surfaces, leading to greater errors than would occur with higher-resolution data such as Landsat TM or ASTER data. Using coarse remote-sensing data in the assimilation procedure introduces a scale disparity between the remotely sensed pixels and the field scale that must be accounted for. Several previous studies confirmed that successful results cannot be obtained by directly assimilating 1-km MODIS LAI and ET values into crop models due to the low values in these products [5], [31], [40]. To solve this issue, we developed a generalized vector angle cost function to allow

assimilation of the temporal variations in the MODIS ET and LAI data rather than assimilating their absolute values into the SWAP model in this study.

In addition to the spatial scale disparity, the temporal disparity between the remote-sensing observations and the modeled outputs also affects the performance of the data assimilation. The MODIS ET and LAI products had 8- and 4-day time intervals, respectively, but the SWAP model generates daily outputs. Thus, a temporal transformation is required to provide consistency of the temporal scale. Furthermore, to obtain more precise crop ET estimates, we need remote-sensing-derived LAI or ET with higher temporal resolution so that daily LAI and ET can be assimilated into the model to improve the model's yield simulation. For example, the two irrigation dates estimated using the SWAP-SCE scheme had errors of $\pm 4$ days due to the 8-day time step in the MODIS ET product.

In this study, we developed a crop model–data assimilation framework for assimilating phenological characteristics from the MODIS ET and LAI time series based on a generalized vector angle cost function. The validation results showed that the estimation accuracy for winter wheat yields improved considerably when assimilating both the MODIS ET and LAI time series. This method does not require field-measured LAI and ET at a regional scale, so it would be easy to extend to applications in other regions. However, this method depends strongly on high-accuracy crop type maps that allow the creation of accurate pixel-purity maps for the study area, because the original MODIS LAI and ET trajectories cannot adequately represent the phenological characteristics of winter wheat in mixed pixels that contain a large proportion of artifacts (e.g., buildings and roads) and other crops with different phenology.

In this study, we selected LAI and ET as the assimilation variables used in the cost function. Additional important state variables (e.g., soil moisture) that are closely related to crop yield should be incorporated into a future DA framework to test the impacts on the estimated crop yield. Hybrid approaches, such as combining the use of EnKF with four-dimensional variational (4-DVar) data assimilation, would allow simultaneous estimation and updating of the model parameters and state variables, and would further improve crop yield simulations at both field and regional scales [41]. In addition, we assigned equal weights to LAI and ET in the cost function developed in the present study. Assigning different weights to ET and LAI at different phenological stages to minimize the impact of observational errors would further improve the assimilation results.

One important application for the crop model–data assimilation system developed in this study would be to predict crop yield before harvesting. However, the accuracy of this application would depend strongly on the accuracy and resolution of the weather data inputs (e.g., precipitation and temperature) for future periods. Several previous studies have implemented crop yield predictions based on different scenarios that used historical weather data from a dry, a wet, and a normal year [42], [43]. However, due to high variability of weather data in the future, this method would inevitably contain relatively large errors. One promising method might be to couple medium-term climate prediction from climate modeling and crop modeling and thus improves the ability of predicting crop yield.

## V. Conclusion

In this study, the SWAP process-based growth model was used to estimate winter wheat yield through incorporating time series of MODIS LAI and ET products using generalized vectorial angle cost function with the SCE-UA optimization algorithm. Generally, crop growth models are subjected to structural and inputs errors. Thus, their simulation for crop growth and yield estimation would deviate from the reality. It was difficult for the SWAP model to simulate the actual crop ET temporal variation with insufficient irrigation data during the growing season. The validation results showed that the MODIS ET or LAI products have the ability to capture the temporal variation of ET or LAI despite the absolute values are underestimated for pure wheat pixels. Validation results show that the generalized vectorial angle cost function approach generates accurate ET or LAI trajectory throughout the growing season and improves the agreement between assimilated ET or LAI and the field-measured ET or LAI. Our results also show that assimilating LAI is more effective than assimilating ET in improving regional wheat yield estimates. By simultaneously assimilating the time series of MODIS LAI and ET products using a generalized vector angle cost function, we were able to greatly improve the accuracy of winter wheat yield estimation at the regional scale. One advantage of the current method is that it can be easily applied in other regions with little or no modification simply by parameterizing the model to account for crop and climatic characteristics. However, the results would be greatly improved by obtaining better parameter values for key factors such as soil moisture and the optimal irrigation schedule and possibly by assimilating data for other factors that affect crop growth and yield (e.g., soil moisture). Remote-sensing data with higher temporal and spatial resolution would also improve the results by improving the tracking of the LAI and ET trajectories.

## Acknowledgment

The authors would like to thank the anonymous reviewers for providing constructive comments and suggestions that improved the quality of this paper.

## References

[1] P. C. Doraiswamy *et al.*, "Crop condition and yield simulations using Landsat and MODIS," *Remote Sens. Environ.*, vol. 92, pp. 548–559, 2004.

[2] H. Fang, S. Liang, and G. Hoogenboom, "Integration of MODIS LAI and vegetation index products with the CSM-CERES-Maize model for corn yield estimation," *Int. J. Remote Sens.*, vol. 32, pp. 1039–1065, 2011.

[3] W. A. Dorigo *et al.*, "A review on reflective remote sensing and data assimilation techniques for enhanced agroecosystem modeling," *Int. J. Appl. Earth Observ. Geoinf.*, vol. 9, pp. 165–193, 2007.

[4] S. Liang and J. Qin, "Data assimilation methods for land surface variable estimation," in *Advances in Land Remote Sensing: System, Modeling, Inversion and Application*, S. Liang, Ed. New York, NY, USA: Springer, 2008, pp. 319–339.

[5] A. de Wit, G. Duveiller, and P. Defourny, "Estimating regional winter wheat yield with WOFOST through the assimilation of green area index retrieved from MODIS observations," *Agric. For. Meteorol.*, vol. 164, pp. 39–52, 2012.

[6] Z. Jiang, "Study of remote sensing data assimilation technology for regional winter wheat yield estimation," Ph.D. dissertation, Chin. Acad. Agric. Sci., Beijing, China, 2012 (in Chinese).

[7] L. Dente, G. Satalino, F. Mattia, and M. Rinaldi, "Assimilation of leaf area index derived from ASAR and MERIS data into CERES-Wheat model to map wheat yield," *Remote Sens. Environ.*, vol. 112, pp. 1395–1407, 2008.
[8] H. Fang, S. Liang, G. Hoogenboom, J. Teasdale, and M. Cavigelli, "Corn-yield estimation through assimilation of remotely sensed data into the CSM-CERES-Maize model," *Int. J. Remote Sens.*, vol. 29, pp. 3011–3032, 2008.
[9] B. Baruth, A. Royer, A. Klisch, and G. Genovese, "The use of remote sensing within the MARS crop yield monitoring system of the European Commission," in *Proc. Int. Soc. Photogramm. Remote Sens. (ISPRS)*, 2008, vol. 37, pp. 935–940.
[10] I. Becker-Reshef, E. Vermote, M. Lindeman, and C. Justice, "A generalized regression-based model for forecasting winter wheat yields in Kansas and Ukraine using MODIS data," *Remote Sens. Environ.*, vol. 114, pp. 1312–1323, 2010.
[11] F. Kogan *et al.*, "Winter wheat yield forecasting in Ukraine based on Earth observation, meteorological data and biophysical models," *Int. J. Appl. Earth Observ. Geoinf.*, vol. 23, pp. 192–203, 2013.
[12] Y. Curnel, A. J. W. de Wit, G. Duveiller, and P. Defourny, "Potential performances of remotely sensed LAI assimilation in WOFOST model based on an OSS Experiment," *Agric. For. Meteorol.*, vol. 151, pp. 1843–1855, 2011.
[13] W. Xu, H. Jiang, and J. Huang, "Regional crop yield assessment by combination of a crop growth model and phenology information derived from MODIS," *Sens. Lett.*, vol. 9, pp. 981–989, 2011.
[14] G. S. Nearing *et al.*, "Assimilating remote sensing observations of leaf area index and soil moisture for wheat yield estimates: An observing system simulation experiment," *Water Resour. Res.*, vol. 48, no. 5, 2012, doi: 10.1029/2011WR011420.
[15] J. W. Jones *et al.*, "The DSSAT cropping system model," *Eur. J. Agron.*, vol. 18, pp. 235–265, 2003.
[16] A. V. Ines, K. Honda, A. Das Gupta, P. Droogers, and R. S. Clemente, "Combining remote sensing-simulation modeling and genetic algorithm optimization to explore water management options in irrigated agriculture," *Agric. Water Manage.*, vol. 83, pp. 221–232, 2006.
[17] W. G. M. Bastiaanssen *et al.*, "SEBAL model with remotely sensed data to improve water-resources management under actual field conditions," *J. Irrig. Drain. Eng.*, vol. 131, pp. 85–93, 2005.
[18] A. Irmak and B. Kamble, "Evapotranspiration data assimilation with genetic algorithms and SWAP model for on-demand irrigation," *Irrig. Sci.*, vol. 28, pp. 101–112, 2009.
[19] M. Vazifedoust, J. C. van Dam, W. Bastiaanssen, and R. A. Feddes, "Assimilation of satellite data into agrohydrological models to improve crop yield forecasts," *Int. J. Remote Sens.*, vol. 30, pp. 2523–2545, 2009.
[20] P. Droogers, W. W. Immerzeel, and I. J. Lorite, "Estimating actual irrigation application by remotely sensed evapotranspiration observations," *Agric. Water Manage.*, vol. 97, pp. 1351–1359, 2010.
[21] S. Charoenhirunyingyos, K. Honda, D. Kamthonkiat, and A. V. M. Ines, "Soil hydraulic parameters estimated from satellite information through data assimilation," *Int. J. Remote Sens.*, vol. 32, pp. 8033–8051, 2011.
[22] G. Duveiller, F. Baret, and P. Defourny, "Crop specific green area index retrieval from MODIS data at regional scale by controlling pixel-target adequacy," *Remote Sens. Environ.*, vol. 115, pp. 2686–2701, 2011.
[23] H. Fang, S. Wei, and S. Liang, "Validation of MODIS and CYCLOPES LAI products using global field measurement data," *Remote Sens. Environ.*, vol. 119, pp. 43–54, 2012.
[24] P. Yang *et al.*, "Evaluation of MODIS land cover and LAI products in cropland of North China Plain using in situ measurements and Landsat TM images," *IEEE Trans. Geosci. Remote Sens.*, vol. 45, no. 10, pp. 3087–3097, Oct. 2007.
[25] Q. Mu, F. A. Heinsch, M. Zhao, and S. W. Running, "Development of a global evapotranspiration algorithm based on MODIS and global meteorology data," *Remote Sens. Environ.*, vol. 111, pp. 519–536, 2007.
[26] L. Kouadio *et al.*, "Estimating regional wheat yield from the shape of decreasing curves of green area index temporal profiles retrieved from MODIS data," *Int. J. Appl. Earth Observ. Geoinf.*, vol. 18, pp. 111–118, 2012.
[27] Q. Mu, M. Zhao, and S. W. Running, "Improvements to a MODIS global terrestrial evapotranspiration algorithm," *Remote Sens. Environ.*, vol. 115, pp. 1781–1800, 2011.
[28] H. W. Kim, K. Hwang, Q. Mu, S. O. Lee, and M. Choi, "Validation of MODIS 16 global terrestrial evapotranspiration products in various climates and land cover types in Asia," *KSCE J. Civ. Eng.*, vol. 16, pp. 229–238, 2012.
[29] Y. Shen and C. Liu, "Agro-ecosystems water cycles of the typical irrigated farmland in the North China Plain," *Chin. J. Eco-Agric.*, vol. 19, pp. 1004–1010, 2011 (in Chinese).
[30] P. Droogers, "Estimating actual evapotranspiration using a detailed agro-hydrological model," *J. Hydrol.*, vol. 229, pp. 50–58, 2000.
[31] G. Ma *et al.*, "Assimilation of MODIS-LAI into the WOFOST model for forecasting regional winter wheat yield," *Math. Comput. Modell.*, vol. 58, pp. 753–764, 2013.
[32] A. Saltelli, S. Tarantola, and K. Chan, "A quantitative model-independent method for global sensitivity analysis of model output," *Technometrics*, vol. 41, pp. 39–56, 1999.
[33] J. Chen *et al.*, "A simple method for reconstructing a high-quality NDVI time-series data set based on the Savitzky–Golay filter," *Remote Sens. Environ.*, vol. 91, pp. 332–344, 2004.
[34] Q. Y. Duan, V. K. Gupta, and S. Sorooshian, "Shuffled complex evolution approach for effective and efficient global minimization," *J. Optim. Theory Appl.*, vol. 76, pp. 501–521, 1993.
[35] Q. Duan, S. Sorooshian, and V. Gupta, "Effective and efficient global optimization for conceptual rainfall–runoff models," *Water Resour. Res.*, vol. 28, pp. 1015–1031, 1992.
[36] Q. Duan, S. Sorooshian, and V. K. Gupta, "Optimal use of the SCE-UA global optimization method for calibrating watershed models," *J. Hydrol.*, vol. 158, pp. 265–284, 1994.
[37] J. R. Dong, C. Y. Zheng, G. Y. Kan, Z. J. Li, and M. Zhao, "Application of SCE-UA approach to economic load dispatch of hydrothermal generation system," *Appl. Mech. Mater.*, vol. 448, pp. 4296–4303, 2014.
[38] X. Song, C. Zhan, and J. Xia, "Integration of a statistical emulator approach with the SCE-UA method for parameter optimization of a hydrological model," *Chin. Sci. Bull.*, vol. 57, pp. 3397–3403, 2012 (in Chinese).
[39] Z. Yuan and Y. Shen, "Estimation of agricultural water consumption from meteorological and yield data: A case study of Hebei, North China," *PLoS One*, vol. 8, 2013. doi:10.1371/journal.pone.0058685.
[40] H. Ma *et al.*, "Estimating regional winter wheat yield by assimilation of time series of HJ-1 CCD NDVI into WOFOST–ACRM model with ensemble Kalman filter," *Math. Comput. Modell.*, vol. 58, pp. 759–770, 2013.
[41] J. Huang *et al.*, "Improving winter wheat yield estimation by assimilation of the leaf area index from Landsat TM and MODIS data into the WOFOST model," *Agric. For. Meteorol.*, vol. 204, pp. 106–121, 2015.
[42] A. J. W. de Wit and C. A. van Diepen, "Crop model data assimilation with the Ensemble Kalman filter for improving regional crop yield forecasts," *Agric. For. Meteorol.*, vol. 146, pp. 38–56, 2007.
[43] C. Yu *et al.*, "Dynamic assessment of the impact of drought on agricultural yield and scale-dependent return periods over large geographic regions," *Environ. Modell. Softw.*, vol. 62, pp. 454–464, 2014.

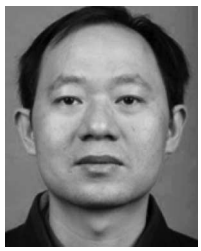

**Jianxi Huang** received the B.Sc. degree in cartography and geographic information system from Wuhan Technical University of Surveying and Mapping, Wuhan, China, in 1999, the M.Sc. degree in cartography and geographic information system from Wuhan University, Wuhan, China, in 2002, and the Ph.D. degree in agricultural remote sensing from the Institute of Remote Sensing Applications, Chinese Academy of Sciences, Beijing, China, in 2006.

Currently, he is an Associate Professor with the College of Information and Electrical Engineering, China Agricultural University, Beijing, China. He has authored more than 20 papers in international journals. His research interests include data assimilation applications in agriculture, crop yield estimation and forecasting, and agricultural drought monitoring and assessment.

**Hongyuan Ma** received the B.Eng. degree in remote sensing science and technology from the School of Remote Sensing and Information of Engineering, Wuhan University, Wuhan, China, in 2011, and the M.Sc. degree in cartography and geographic information system from the College of Information and Electrical Engineering (CIEE), China Agricultural University (CAU), Beijing, China, in 2013. Currently, he is pursuing the Ph.D. degree in agricultural remote sensing at CIEE.

His research interests include agricultural remote sensing, data assimilation, and crop model simulation.

**Wei Su** received the B.Sc. degree in land management and the M.Sc. degree in cartography and geographic information system from Shandong Agricultural University, Tai'an, China, in 2001 and 2004, respectively, and the Ph.D. degree in cartography and geographic information system from Beijing Normal University, Beijing, China, in 2007.

Currently, she is an Associate Professor with the China Agricultural University, Beijing, China. She has authored more than 10 papers in international journals. Her research interests include 3-D radiative transfer models of the vegetation canopy and crop growth monitoring.

**Xiaodong Zhang** received the B.Sc. degree in physical geography from Beijing Normal University, Beijing, China, in 1988, the M.S. degree in physical geography from Peking University, Beijing, China, in 1993, and the Ph.D. degree in cartography and geographic information system from the Institute of Geographic Sciences and Natural Resources Research, Chinese Academy of Science, Beijing, China, in 2000.

Currently, she is a Professor with China Agricultural University, Beijing, China. Her research interests include remote sensing for disaster monitoring, and GIS applications and information technology in agriculture.

**Yanbo Huang** received the B.Eng. degree from Beijing University of Science and Technology, Beijing, China, in 1983, the M.Eng. degree from Chinese Academy of Mechanics and Electronics Sciences, Beijing, China, in 1986, both in industrial automation, and the Ph.D. degree in agricultural engineering from Texas A&M University, College Station, TX, USA, in 1995.

Currently, he is a Senior Research Agricultural Engineer with United Department of Agriculture (USDA), Agricultural Research Service (ARS), Stoneville, MS, USA. He is an Adjunct Professor with Texas A&M University, Mississippi State University, Starkville, MS, USA, and Delta State University, Cleveland, MS, USA, and the Guest Research Fellow with Chinese Academy of Agricultural Science, Beijing, China.

Dr. Huang is an Editor-In-Chief of *International Journal and Agricultural Science and Technology* (IJAST), Section Editor of *International Journal of Agricultural and Biological Engineering* (IJABE), and Associate Editor of *Transactions of the American Society of Agricultural and Biological Engineers* (ASABE).

**Jinlong Fan** received the B.Sc.degree in soil science and agricultural chemistry from Shanxi Agricultural University, Jinzhong, China, in 1996, the M.Sc. degree in agricultural meteorology from China Agricultural University, Beijing, China, in 2000, and the Ph.D. degree in agricultural remote sensing from the Institute of Remote Sensing Applications, Chinese Academy of Sciences, Beijing, China, in 2003.

Currently, he is an Associate Professor with National Satellite Meteorological Center, Beijing, China. His research interests include processing of low-resolution satellite data and quick responses to disaster monitoring, as well as agricultural monitoring by means of remote sensing.

**Wenbin Wu** received the B.S. degree in geography from HuaZhong Normal University, Hubei, China, in 1998, the M.Eng. degree in environmental engineering from Chinese Academy of Agriculture Sciences, Beijing, China, in 2005, and the Ph.D. degree in agricultural spatial informatics from the University of Tokyo, Tokyo, Japan, in 2008.

Currently, he is a Research Professor with the Institute of Agricultural Resources and Regional Planning, Chinese Academy of Agricultural Sciences. His research interests include agricultural remote sensing, monitoring and modeling of changes in agricultural land systems by integrating remote sensing, GIS, and statistical methodologies.